CellPress
PARTNER JOURNAL

Molecular Plant
Letter to the Editor

Microrheological Insights into the Dynamics of Amyloplasts in Root Gravity-Sensing Cells

Dear Editor,

Gravitropism in plants is key for orienting organs such as the Darwin's description of the opposite growth direction of roots and shoots in his book *The Power of Movement in Plants* more than 100 years ago (Darwin, 1880). The gravitropic response of an oriented plant is divided into three sequential phases: gravity sensing, signal transmission, and the growth response. As the initial phase of gravitropism, gravity sensing (the conversion of the mechanical stimulus into a biochemical signal) has been intensively studied, but much is still unknown. The statoliths are vital for sense of balance and response to gravity, e.g. in statocytes for invertebrates and in inner ears for vertebrates. The most widely accepted starch–statolith hypothesis proposes that the physical sedimentation of amyloplasts (statoliths in plants) in the direction of gravity in gravity-sensing cells, such as root columella cells and shoot endodermal cells, triggers biochemical signals (Morita, 2010). The physical movement of amyloplasts in gravity-sensing cells is believed to primarily trigger auxin asymmetric distribution, leading to differential growth across the organ during the gravitropic response (Vanneste and Friml, 2009). It has been gradually recognized that the interaction between amyloplasts and the surrounding intracellular components, e.g. the cytoskeleton and vacuole, greatly affects the Brownian diffusion of amyloplasts leading to a complexity in amyloplast movement (Hou et al., 2004; Leitz et al., 2009).

In the past decade, microrheology become a powerful tool to explore relationships between local mechanical responses and structures in inhomogeneous fluids. Microrheology analyses have been applied *in vitro* to quantitatively evaluate the mechanical functions of the cytoskeletal network during cell locomotion and cell division (Chaudhuri et al., 2007; Mizuno et al., 2007; Wirtz, 2009). Amyloplast movement in gravity-sensing cells provides a useful tool (amyloplasts as the native micro-sized probes) for probing the heterogeneous intracellular environment *in vivo*. Using a rotatable stage, amyloplast sedimentation in central columella cells of *Arabidopsis* wild-type plants (ecotype Columbia, Col) was recorded by time-lapse video microscopy. After a 90° reorientation, most of the amyloplasts fell to the new bottom side of columella cells within 400 s (Figure 1A and Supplemental Movie 1). We plotted the movement trajectory of each amyloplast to analyze their Brownian dynamics by single-particle tracking and subtracting the collective sedimentation (Figure 1B). The trajectory of an amyloplast showed a chain-like pattern with a constant small-step motion and an occasional large-step motion, the typical characteristics of the cage effect on particle diffusion that generally exists in dense colloidal suspensions (Zheng et al., 2011, 2014). The localized small-step rattling motion corresponds to the confined Brownian motion within cages, while the chain-like large-step motion corresponds to the cooperative out-of-cage motion of several amyloplasts (Supplemental Movie 2). These results suggest that there is a colloidal-like intracellular environment with highly spatial heterogeneity in the columella cells, where amyloplast sedimentation is facilitated by intermittent collective cage-escape processes.

Mean square displacement (MSD) was used for analysis of amyloplast displacement in shoot gravity-sensing cells (Toyota et al., 2013). Here, the diffusive dynamics of amyloplasts in root columella cells during sedimentation were quantitatively measured by the MSD against the time interval t as follows: $MSD_{x,y}(t) = \langle \Delta r_{x,y}(t)^2 \rangle - \langle \Delta r_{x,y}(t) \rangle^2$, where $\Delta r_{x,y}$ is the displacement of an amyloplast in the horizontal (x axis) or gravitational (y axis) direction. The typical log–log plot of the MSD of all amyloplasts in a wild-type columella cell (Figure 1C) is divided into three time regimes. (1) In the initial regime, the log–log MSD had a unit slope, i.e. a linear increase against t, reflecting the short-time Brownian diffusion of amyloplasts with a random rattling motion before they encounter cages. (2) In the intermediate regime, the MSD develops a plateau deviating downward from the unit slope, reflecting the cage confinement of amyloplast diffusion exerted by the surrounding circumstances. (3) In the final regime, the MSD returns to a unit slope, indicating the regaining of diffusive motion after amyloplasts break out of the cages. The long-time diffusion corresponds to the long-distance collective rearrangement of amyloplasts, which occurs more slowly than does the short-time in-cage diffusion. The cage-confined diffusion in the intermediate regime was further confirmed by the long tails in the distribution of the amyloplast displacements. These long tails corresponded to the appearance of the large-step cage-escape motion, and resulted in the deviation from Gaussian distribution for normal random diffusion (Supplemental Figure 1).

To quantitatively depict the intracellular structural heterogeneity, we measured the local apparent viscosity in the columella cells. According to the fluctuation–dissipation theory, the local viscosity η is obtained from the Brownian diffusion of microprobes following the Stokes–Einstein relation: $D = MSD(t)/(2t) = k_B T/(6\pi R\eta)$ (Wirtz, 2009), where D is the short-time diffusion coefficient of a microprobe with radius R, k_B is Boltzmann's constant, and T is temperature. The columella cell was divided into nine subregions to provide an accurate description of spatial heterogeneity (Figure 1F, inset). The local viscosity fluctuated, ranging from ~0.02 to ~0.1 Pa s^{-1}, indicating that there is remarkable spatial heterogeneity and anisotropy in the intracellular environment (Figure 1E).

Published by the Molecular Plant Shanghai Editorial Office in association with Cell Press, an imprint of Elsevier Inc., on behalf of CSPB and IPPE, SIBS, CAS.

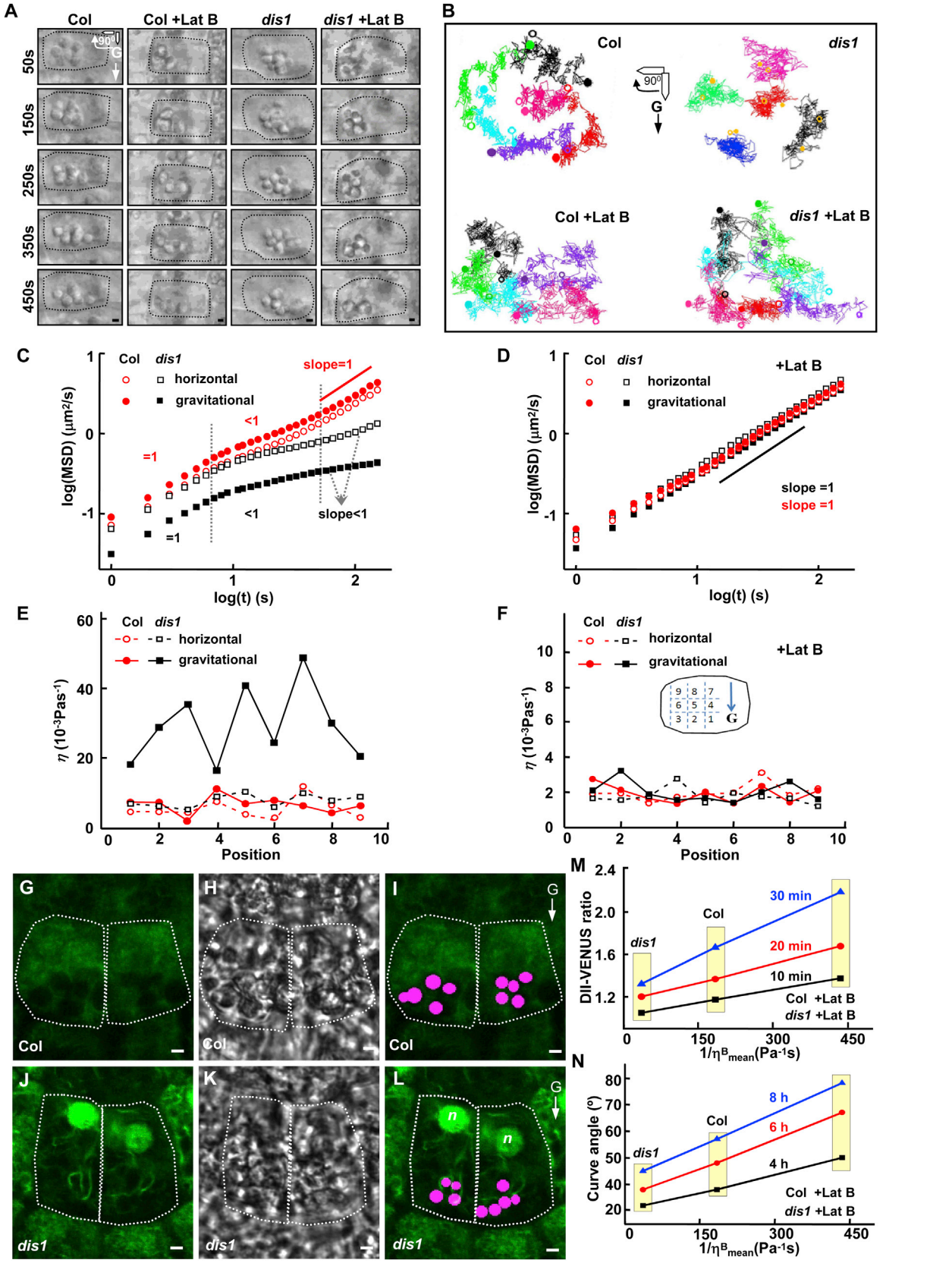

(legend on next page)

The filamentous actin (F-actin) network in columella cells was visualized using Alexa Fluor-phalloidin dyes after glycerol permeation (Le et al., 2003). Consistent with previous results (Hou et al., 2004), only diffuse fluorescence was observed in central columella cells, in contrast to the actin bundles exhibited in the adjacent peripheral columella cells (Figure 1G–1I and Supplemental Movie 3). Amyloplasts are located in actin hollows, which may form the cages confining them. However, columella cells pretreated with the actin-disrupting drug latrunculin (Lat) B (1 h) showed an accelerated amyloplast sedimentation within 300 s (Figure 1A and Supplemental Movie 4) and displayed homogeneous and overlapped trajectories (Figure 1B). The MSD of amyloplasts in Lat B-treated columella cells showed a linear relationship with time (Figure 1D), which is a feature of free diffusive motion without cage confinement. This is consistent with the greatly decreased local viscosity (Figure 1F).

Mutation of the *DISTORTED1* (*DIS1*) gene, which encodes the Actin Related Protein 3 (ARP3) subunit of the ARP2/3 complex, induces the formation of misorganized thick actin bundles (Le et al., 2003). In agreement with the defective root response to gravitropic stimulation (Supplemental Figure 2), *dis1* columella cells displayed retarded amyloplast sedimentation with a typical duration of approximately 600 s (Figure 1A and Supplemental Movie 5). The amyloplasts in *dis1* rattled randomly within separate cages with relatively fixed positions and no overlaps, but did not undergo a cooperative cage escape, indicating stronger cage confinement in *dis1* (Figure 1B and Supplemental Movie 6). The MSD in *dis1* is lower and plateaus longer than that of Col, and long-time diffusion was not regained (Figure 1C). The local viscosity in the horizontal direction was similar to that of the wild-type, while the mean value and spatial fluctuation of local viscosity in the gravitational direction were approximately five times higher in *dis1* than that in Col (Figure 1E). Different from the wild-type, actin bundles surrounding amyloplasts were present in the *dis1* central columella cells (Figure 1J–1L and Supplemental Movie 7). However, after treatment with Lat B, the *dis1* columella cells showed similar amyloplast sedimentation, trajectories, MSD, and local viscosity behavior compared with that of the wild-type (Figure 1A, 1B, 1D, and 1F; Supplemental Movie 8). Therefore, the strength of mechanical confinement to amyloplasts was consistent with the structural heterogeneity of the actin cytoskeleton in the columella cells. These results confirm the dominance of actin-cytoskeletal structures in the intracellular microenvironments of central columella cells that determine the sedimentation dynamics of amyloplasts.

It is thought that sedimentary amyloplasts cause strain deformation of unknown acceptor components that may activate a biochemical signal, such as auxin. The strain deformation can be equivalently measured from the net kinetic momentum (impulse) of the sedimentary amyloplasts $L = m_{mean} v_{mean}$, where m_{mean} and v_{mean} are the mean mass and mean instantaneous velocity along gravity direction of amyloplast in the columella cell, respectively. Since the mean mass of amyloplasts is almost identical in the Col, *dis1*, and Lat B-treated columella cells, L is proportional to the average velocity of amyloplasts v_{mean}, which is inversely proportional to the resistance of actin cytoskeleton measured by the inverse mean viscosity $1/\eta^{B}_{mean}$ (usually called actin cytoskeleton fluidity; see the detailed method in Supplemental Information). To monitor the auxin asymmetry after gravity stimulation, we measured the 35S::DII-VENUS-N-N7 (Band et al., 2012) signal ratio between the upper and lower sides cells adjacent to the columella cells (Supplemental Figure 3). Interestingly, the DII-VENUS ratios and the root curvatures at different times showed almost linear increases with $1/\eta^{B}_{mean}$(Figure 1M and 1N). These results suggest the presence of a gravity-sensing mechanism that harbors a linear frustration effect of the actin cytoskeleton on the conversion of mechanical stimulation from amyloplasts into gravitropic signals. Such linear relationships between mechanical stimulation by amyloplasts, the asymmetric distribution of auxin, and root curvature, collectively support a model that directly links initial intracellular gravity sensing, subsequent intercellular signal transmission, and the final gravity response.

SUPPLEMENTAL INFORMATION

Supplemental Information is available at *Molecular Plant Online*.

FUNDING

This work was supported by the National Basic Research Program of China (Grant No. 2011CB710902 and 2011CB710901) and National Natural Science Foundation of China (Grant No. 11104286 and 11372314).

ACKNOWLEDGMENTS

We thank Fred Sack for discussion and providing DII-VENUS seeds; Dan Szymanski for dis mutants. No conflict of interest declared.

Figure 1. The Biomechanical Analysis of Amyloplast Sedimentation in Gravity-Sensing Cells.

(A) Time-lapse images of amyloplast sedimentation in the central columella cells after 90° reorientation. Untreated Col (wild-type), *dis1* (actin mutant), and actin-disrupting drug Lat B-treated Col and *dis1*.

(B) Movement trajectories of amyloplasts in the central columella cells after 90° reorientation. The solid and open circles denote the start and the end point of each amyloplast, respectively.

(C and D) Diffusive motions of amyloplasts are characterized by typical log–log MSD(t) during sedimentation in horizontal and gravitational directions. Untreated Col and *dis1* displayed distinct slopes at different time phases **(C)**. There were no differences between Lat B-treated Col and *dis1* **(D)**.

(E and F) Apparent local viscosity within gravity-sensing cells. The inset in **(F)** illustrates the nine subregions of central columella cells. Here "gravitational" and "horizontal" mean the directions along and perpendicular to the gravitational force denoted by arrow G.

(G–L) Organization of actin cytoskeleton in the central columella cells of Col **(G–I)** and *dis1* **(J–L)**. **(G)** and **(J)** are confocal images of F-actin in fixed roots labeled with Alexa Fluor-phalloidin (Le et al., 2003). In contrast to the diffuse fluorescence in wild-type, *dis1* columella cells contain thick F-actin bundles. **(H)** and **(K)** are bright-field images of same cells. Cell outline is indicated by dashed lines. The magenta dots in **(I)** and **(L)** indicate the location of amyloplasts. Dense actin patches surrounding nucleus were often observed in *dis1* (n).

(M and N) The linear relationship between the inverse mean viscosity $1/\eta^{B}_{mean}$ and DII-VENUS ratios **(M)** or root curvature angle **(N)**. DII-VENUS ratios are measured in lateral root cap cells adjacent to the columella cells between the upper and lower sides of roots at different times after 90° reorientation of the plants. η^{B}_{mean} is averaged over subregions that are adjacent to the new cell bottom wall within the columella cells.

Scale bars represent 2 μm.

Received: October 23, 2014
Revised: December 20, 2014
Accepted: December 29, 2014
Published: January 5, 2015

Zhongyu Zheng[1,3], *Junjie Zou*[2,3], *Hanhai Li*[1], *Shan Xue*[2], *Yuren Wang*[1,*] and *Jie Le*[2,*]

[1]Key Laboratory of Microgravity, Institute of Mechanics, Chinese Academy of Sciences, Beijing 100190, China
[2]Key Laboratory of Plant Molecular Physiology, Institute of Botany, Chinese Academy of Sciences, Beijing 100093, China
[3]These authors contributed equally to this article.
***Correspondence: Jie Le (lejie@ibcas.ac.cn), Yuren Wang (yurenwang@imech.ac.cn)**
http://dx.doi.org/10.1016/j.molp.2014.12.021

REFERENCES

Band, L.R., Wells, D.M., Larrieu, A., Sun, J., Middleton, A.M., French, A.P., Brunoud, G., Sato, E.M., Wilson, M.H., Péret, B., et al. (2012). Root gravitropism is regulated by a transient lateral auxin gradient controlled by a tipping-point mechanism. Proc. Natl. Acad. Sci. USA **109**:4668–4673.

Chaudhuri, O., Parekh, S.H., and Fletcher, D.A. (2007). Reversible stress softening of actin networks. Nature **445**:295–298.

Darwin, C. (1880). The Power of Movement in Plants (London: John Murray).

Hou, G., Kramer, V.L., Wang, Y.-S., Chen, R., Perbal, G., Gilroy, S., and Blancaflor, E.B. (2004). The promotion of gravitropism in *Arabidopsis* roots upon actin disruption is coupled with the extended alkalinization of the columella cytoplasm and a persistent lateral auxin gradient. Plant J. **39**:113–125.

Le, J., El-Assal Sel, D., Basu, D., Saad, M.E., and Szymanski, D.B. (2003). Requirements for *Arabidopsis* ATARP2 and ATARP3 during epidermal development. Curr. Biol. **13**:1341–1347.

Leitz, G., Kang, B.-H., Schoenwaelder, M.E.A., and Staehelin, L.A. (2009). Statolith sedimentation kinetics and force transduction to the cortical endoplasmic reticulum in gravity-sensing *Arabidopsis* columella cells. Plant Cell **21**:843–860.

Mizuno, D., Tardin, C., Schmidt, C.F., and Mackintosh, F.C. (2007). Nonequilibrium mechanics of active cytoskeletal networks. Science **315**:370–373.

Morita, M.T. (2010). Directional gravity sensing in gravitropism. Annu. Rev. Plant Biol. **61**:705–720.

Toyota, M., Ikeda, N., Sawai-Toyota, S., Kato, T., Gilroy, S., Tasaka, M., and Morita, M.T. (2013). Amyloplast displacement is necessary for gravisensing in *Arabidopsis* shoots as revealed by a centrifuge microscope. Plant J. **76**:648–660.

Vanneste, S., and Friml, J. (2009). Auxin: a trigger for change in plant development. Cell **136**:1005–1016.

Wirtz, D. (2009). Particle-tracking microrheology of living cells: principles and applications. Annu. Rev. Biophys. **38**:301–326.

Zheng, Z., Wang, F., and Han, Y. (2011). Glass transitions in quasi-two-dimensional suspensions of colloidal ellipsoids. Phys. Rev. Lett. **107**:065702.

Zheng, Z., Ni, R., Wang, F., Dijkstra, M., Wang, Y., and Han, Y. (2014). Structural signatures of dynamic heterogeneities in monolayers of colloidal ellipsoids. Nat. Commun. **5**:3829.